Eur. Phys. J. D **46**, 69–76 (2008)
DOI: 10.1140/epjd/e2007-00285-3

THE EUROPEAN PHYSICAL JOURNAL D

Simulating CH_4 physisorption on ionic crystals

Limitations of an atomic partial charge model

P.J. Stimac[a] and R.J. Hinde[b]

Department of Chemistry, University of Tennessee, Knoxville, TN 37996-1600, USA

Received 18 April 2007 / Received in final form 11 September 2007
Published online 10 October 2007 –

Abstract. We use quantum chemical techniques to evaluate the electrostatic and polarization components of the interaction between a rigid CH_4 molecule and a lattice of point charges representing the MgO(100) surface. We find that CH_4 positioned above Mg adopts an edge-down configuration in which two H atoms are oriented downward towards the MgO(100) surface and point at O ions in the surface layer. The CH_4–MgO(100) electrostatic interaction is substantially less favorable (but is still attractive) for the face-down configuration in which three H atoms point downward. Neither configuration is energetically favorable for CH_4 molecules positioned above O ions. We show that for edge-down CH_4 molecules above Mg, the electrostatic component of the CH_4-substrate interaction varies considerably as the CH_4 molecule rotates about the surface normal; the polarization component of the interaction, by contrast, is nearly constant during this rotation. We show that a point-charge model for the CH_4 charge distribution, in which the C and H atoms carry effective partial charges, predicts that the CH_4-surface electrostatic interaction should be more favorable for face-down CH_4 molecules than for edge-down CH_4 molecules, in disagreement with the quantum chemical results. We show that this is because the point-charge model poorly represents the high-order electric multipoles of CH_4.

PACS. 33.15.Kr Electric and magnetic moments (and derivatives), polarizability, and magnetic susceptibility – 68.47.Gh Oxide surfaces – 68.43.Fg Adsorbate structure (binding sites, geometry)

1 Introduction

The interaction of CH_4 adsorbates with the (100) surfaces of rocksalt-structure ionic solids has been a topic of considerable interest for many years [1–19]. One of the most fundamental questions regarding the CH_4-substrate interaction involves the configuration adopted by the CH_4 adsorbates. Deprick and Julg [1,2] were among the first to try to determine this configuration using ab initio quantum chemical methods. They considered a CH_4 adsorbate suspended above a finite lattice of point charges representing either the MgO(100) or the NaCl(100) surface, and computed the energy of the adsorbate at the Hartree-Fock (HF) level of theory using a relatively small basis set consisting of s and p atom-centered Gaussian orbitals. This study suggested that on both MgO(100) and NaCl(100) surfaces, the edge-down adsorption configuration, in which two hydrogen atoms point towards the substrate and the CH_4 adsorbate's two-fold rotational symmetry axis is perpendicular to the surface, was more stable than the face-down configuration, in which three hydrogen atoms point towards the substrate and the CH_4 adsorbate's three-fold rotational symmetry axis is oriented perpendicular to the surface.

Later quantum chemical studies [15] of CH_4 adsorbates on MgO(100) employed an embedded cluster model for the MgO(100) surface and incorporated electron correlation effects. This model considered explicitly the electronic structure of both the CH_4 adsorbate and a small set of Mg and O atoms near the adsorbate. These substrate Mg and O atoms were surrounded by a small array of ab initio model potentials, and the entire system was embedded in a Madelung potential representing an infinite lattice of point charges. Like the earlier quantum chemical investigations, these studies also predicted that the edge-down configuration was more stable than the face-down configuration. However, the later ab initio studies suggested that the binding energy of the edge-down CH_4 adsorbate was due almost entirely to dispersion or van der Waals interactions. For example, at the HF level of theory, which includes both electrostatic and induction contributions to the adsorption energy, the edge-down binding energy for an isolated CH_4 adsorbate was estimated to be only 2 meV from a calculation that employed s and p Gaussian orbitals on the CH_4 atoms. A correlated calculation employing the same atomic basis set gave an edge-down binding energy of 27 meV. A correlated calculation using a

[a] *Current address:* Department of Chemistry, University of Montana, Missoula, MT 59812, USA.
[b] e-mail: rhinde@utk.edu

larger atomic basis set gave an edge-down binding energy of about 40 meV; after the application of empirical corrections for incompleteness in the one- and many-electron basis sets, the edge-down binding energy estimated in this study rose to about 55 meV.

A more recent density functional quantum chemical investigation [19] of adsorption of CH_4 monolayers on the MgO(100) surface also found that the edge-down adsorption configuration was more stable than the face-down configuration. This study treated the electronic structure of both the CH_4 adsorbate monolayer and the MgO(100) surface using the PW91 [20,21] density functional; this approach thus includes some effects of electron correlation, although the question of whether long-range dispersion interactions are treated accurately using the PW91 functional is still a matter of debate. This study found that the per-molecule adsorption energy of a monolayer of adsorbed CH_4 was 18 meV for edge-down CH_4 molecules adsorbed in "herringbone" fashion [22].

Several investigations [3,5,15] of the structure and dynamics of CH_4 monolayers adsorbed on MgO(100) have employed empirical CH_4–MgO(100) interaction potentials. When these empirical potentials have included the CH_4–MgO(100) electrostatic interaction [5,15], they have done so using a point-charge model for the CH_4 charge distribution, in which the four H atoms have fractional positive effective charges and the C atom acquires a fractional negative effective charge to maintain charge neutrality of the CH_4 molecule. In contrast to the quantum chemical calculations, these empirical potentials predict the face-down adsorption configuration to be more stable than the edge-down configuration.

Recent inelastic neutron scattering experiments [13,16,18] that probe the rotational tunneling transitions of CH_4 molecules in a monolayer film adsorbed on MgO(100) at $T = 1.5$ K have been interpreted [18] as indicating that the adsorbates adopt the edge-down configuration at this temperature. The CH_4 rotational tunneling splittings contain information on the topography of the CH_4–MgO(100) interaction potential; this information can in principle be extracted from the splittings with the help of quantum dynamical simulations of the hindered rotor states of the CH_4 adsorbates. However, these simulations require as input a reasonably accurate six-dimensional CH_4–MgO(100) potential energy surface, and such a surface has not yet been developed.

Toward this end, we report here ab initio quantum chemical calculations of the interaction between an isolated CH_4 adsorbate and a finite lattice of point charges intended to mimic the MgO(100) substrate. Our computational approach allows us to isolate the electrostatic component of the CH_4–lattice interaction energy; we show that for both edge-down and face-down CH_4 adsorbates, this component can be evaluated quantitatively in terms of the multipole moments of the CH_4 molecule, provided that values for CH_4 multipoles up through the 2^8-pole are available. We explain why the empirical CH_4–MgO(100) potential energy functions that employ a point-charge model for the CH_4 charge distribution find the face-down adsorption configuration to be more stable than the edge-down configuration, and we show that this result originates in the fact that a point-charge model for CH_4 does not represent the molecule's high-order multipoles very well. We therefore recommend that future simulations of CH_4 adsorption on ionic solids should abandon point-charge representations of the CH_4 charge distribution and instead employ accurate ab initio CH_4 multipole moments.

2 Ab initio calculations

We begin by describing the ab initio quantum chemical methods we use to investigate the interaction between CH_4 and a lattice of point charges. The point charge lattice is constructed so as to reproduce the electric field $\mathbf{F} = -\nabla\varphi$ associated with the potential φ above the MgO(100) substrate; this potential is given by equation (2.9.16) of reference [23]:

$$\varphi(X,Y,Z) = \frac{Q}{4\pi\epsilon_0}\frac{16}{\sqrt{2}a}\left(\frac{e^{-\sqrt{8}\pi Z/a}}{1+e^{-\pi\sqrt{2}}}\right) \times \cos\bigl(2\pi X/a\bigr)\cos\bigl(2\pi Y/a\bigr). \quad (1)$$

Here Q is the charge on Mg substrate ions and $a = 7.98a_0$ is twice the nearest-neighbor Mg–O distance in the MgO solid. The capital letters X, Y, and Z represent Cartesian coordinates in a frame of reference defined by the the MgO(100) surface. In this frame of reference, the X and Y axes are aligned with nearest-neighbor Mg–O pairs and the positive Z axis points away from the MgO(100) surface. The origin $(X,Y,Z) = (0,0,0)$ is chosen to be a surface-layer Mg ion. We should emphasize that equation (1) is valid in the approximation that the Mg and O ions are spherical and that the point (X,Y,Z) is outside the substrate charge distribution.

To approximate φ in the region above the MgO(100) substrate, we construct a finite square bilayer of point charges located at Mg and O lattice sites. The first layer is at $Z = 0$ and contains $83 \times 83 = 6889$ point charges; the central charge in this layer represents the Mg ion at $(X,Y,Z) = (0,0,0)$ and carries charge Q. Underneath this layer is a second layer, also with 6889 point charges, centered at $(X,Y,Z) = (0,0,-a/2)$; the point charge at this location represents an O ion and carries charge $-Q$. To confirm that this bilayer mimics the MgO(100) surface electric field accurately, we evaluate the Cartesian components of the bilayer field at 66 points with $Z = 2.5$ Å and $0 \le X \le Y \le a$, and compare these components to those computed by differentiating equation (1). We find that the Cartesian components of the bilayer field agree with those obtained from equation (1) to an accuracy of better than 1%.

We position a CH_4 molecule above the central Mg ion, oriented either edge-down or face-down, with the C atom located at $(X,Y,Z) = (0,0,h)$. For the edge-down CH_4 molecule, two H atoms are located at $(X,Y,Z) = (0,\pm b\sqrt{2/3}, h + b/\sqrt{3})$ and two H atoms are located at

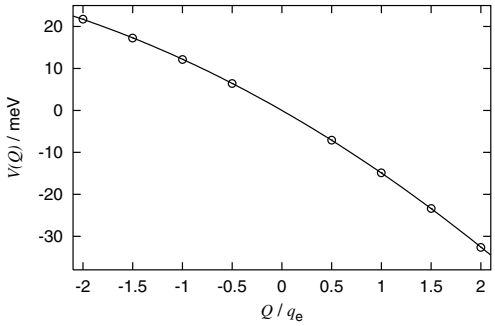

Fig. 1. Dependence of the ab initio CH_4–lattice interaction energy V on the charge Q for edge-down CH_4 with $h = 3.5$ Å. The open circles are the ab initio interaction energies; the solid line is a quadratic fit ($V = sQ + pQ^2$) to these points.

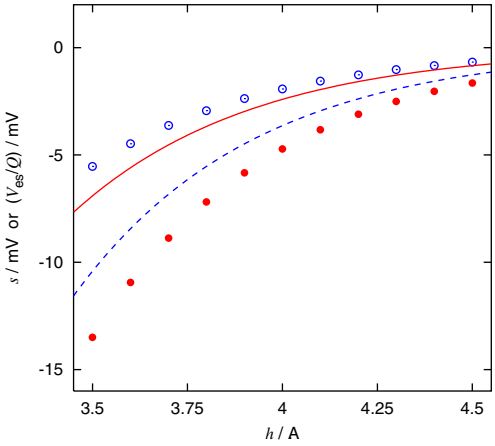

Fig. 2. Dependence on the CH_4 height h of both the ab initio CH_4–lattice electrostatic interaction coefficient s and the substrate-charge-normalized interaction V_{es}/Q [Eq. (2)]. Open and filled circles represent s for face-down and edge-down adsorbates, respectively; dashed and solid curves represent V_{es}/Q for face-down and edge-down adsorbates, respectively.

$(X, Y, Z) = (\pm b\sqrt{2/3}, 0, h - b/\sqrt{3})$, where $b = 2.0518a_0$ is the equilibrium CH bond length [24]. For the face-down molecule, one H atom is located at $(X, Y, Z) = (0, 0, h+b)$, one is at $(X, Y, Z) = (b\sqrt{8/9}, 0, h - b/3)$, and two are at $(X, Y, Z) = (-b\sqrt{2/9}, \pm b\sqrt{2/3}, h - b/3)$. We then use Gaussian 03 [25] to compute the total energy of the CH_4 molecule in the presence of the point charges, and subtract from this the total energy of the isolated CH_4 molecule to obtain V, the interaction between the CH_4 molecule and the point charge lattice. Both total energy computations are performed at the HF level of theory using the aug-cc-pCVTZ atom-centered basis set for C and the aug-cc-pVTZ basis set for H [26–28]; at this level of theory, the total energy of the isolated CH_4 molecule is $E = -40.2138242$ au. (Note that the internal geometry of the CH_4 molecule is held fixed at its equilibrium tetrahedral configuration in all of the calculations reported here.) The interaction energy V is computed for several values of Q between $-2q_e$ and $+2q_e$.

Figure 1 shows how the ab initio CH_4–lattice interaction V depends on Q for edge-down CH_4 molecules at $h = 3.5$ Å. The interaction energy is well fit by a quadratic equation in Q, $V(Q) = sQ+pQ^2$, where sQ represents the electrostatic interaction between the point charge lattice and the CH_4 molecule and pQ^2 represents the induction energy arising from polarization of the CH_4 molecule by the electric field of the lattice. For the data shown in Figure 1, $s < 0$, which indicates that the electrostatic interaction between an edge-down CH_4 molecule and the point charge lattice is favorable when the molecule is positioned above a positive surface-layer ion (and unfavorable when CH_4 is above a negative surface-layer ion).

Figure 2 shows how the electrostatic interaction coefficient s for edge-down and face-down CH_4 adsorbates depends on the adsorbate height h. (The coefficient p representing the polarization interaction is relatively small for both adsorption configurations and decays rapidly with increasing h; at $h = 3.5$ Å, $p = -0.82$ mV/q_e and -1.36 mV/q_e for face-down and edge-down molecules, respectively. This indicates that for realistic values of Q, the ab initio interaction energy is dominated by the electrostatic component.) Also shown in Figure 2 is the substrate-charge-normalized electrostatic interaction

$$\frac{V_{es}}{Q} = \frac{1}{Q}\sum_{i=1}^{5} q_i \varphi(X_i, Y_i, Z_i) \qquad (2)$$

between the MgO(100) substrate and a point-charge model of the (edge-down or face-down) CH_4 adsorbate. In this point-charge model for CH_4, the effective charge q on each H atom is taken to be $q = 0.143q_e$ and the effective charge on the C atom is taken to be $-4q$; the coordinates (X_i, Y_i, Z_i) of the C and H atoms were defined above for edge-down and face-down CH_4 molecules. As noted previously, this point-charge model for the electrostatic component of the CH_4–MgO(100) interaction has been used in earlier classical [5] and quantum mechanical [14] studies of the dynamics of CH_4 monolayers on MgO(100), studies which found the most stable configuration for CH_4 to be face-down above Mg.

We see from Figure 2 that the ab initio calculations predict that the electrostatic component of the CH_4–MgO(100) interaction stabilizes the edge-down configuration with respect to the face-down configuration. The relative stabilities of these two configurations are reversed, however, when the point-charge model for CH_4 is used to compute the CH_4–MgO(100) electrostatic interaction; this is in accord with the results of the earlier dynamical studies [5,14]. The discrepancy between the ab initio results and those of the point-charge model originates in the fact that the point-charge model is an unfaithful representation of the high-order multipole moments of the CH_4 molecule. To demonstrate this, we turn our attention to these multipole moments.

Table 1. Primitive Cartesian multipole moments $P_{i,j,k}$, in atomic units, for CH_4 at the Hartree-Fock (HF) and coupled-cluster singles-and-doubles (CCSD) levels of theory.

(i,j,k)	HF	CCSD
(1, 1, 1)	0.974	1.013
(4, 0, 0)	–44.089	–44.451
(2, 2, 0)	–13.214	–15.360
(6, 0, 0)	–441.014	–450.911
(4, 2, 0)	–101.371	–103.626
(2, 2, 2)	–33.584	–34.487
(5, 1, 1)	–119.326	–120.344
(3, 3, 1)	–69.251	–69.978
(8, 0, 0)	–6868.103	–7283.087
(6, 2, 0)	–1188.802	–1255.169
(4, 4, 0)	–753.107	–794.449
(4, 2, 2)	–276.050	–291.205

3 CH_4 electrical properties

The charge distribution within the CH_4 molecule is characterized by the primitive Cartesian multipole moments

$$P_{i,j,k} = \int x^i y^j z^k \rho(\mathbf{r}) \mathrm{d}\mathbf{r} \tag{3}$$

where $\rho(\mathbf{r})$ is the molecule's charge density (including both electronic and nuclear contributions) and i, j, and k are non-negative integers. In equation (3), the C nucleus is taken as the origin of the (x, y, z) Cartesian coordinate system.

When the CH_4 molecule is oriented with its two-fold rotational axes along the x-, y-, and z-axes and one CH bond along the vector $(1, 1, 1)$, symmetry considerations force $P_{i,j,k}$ to vanish unless i, j, and k are either all even or all odd integers. Table 1 lists several primitive multipole moments for the CH_4 molecule in this orientation, which we refer to as the *standard orientation* henceforth; these moments were calculated using Dalton 1.2.1 [29] at both the HF and coupled-cluster [30,31] singles-and-doubles [32] levels of theory, employing the same atom-centered basis sets and CH bond length given above. Note that in the standard orientation, $P_{i,j,k}$ is invariant under any permutation of its subscripts.

The Cartesian tensor multipole moments of the CH_4 molecule are defined via

$$M_{\alpha\beta\gamma\ldots} = \frac{(-1)^n}{n!} \int r^{2n+1} \left[\frac{\partial^n}{\partial r_\alpha \partial r_\beta \partial r_\gamma \cdots} \left(\frac{1}{r} \right) \right] \rho(\mathbf{r}) \mathrm{d}\mathbf{r}. \tag{4}$$

The tensor moment M with n indices is termed the 2^n-pole moment; there are simple algebraic relations between the individual components of this moment and the primitive Cartesian moments $P_{i,j,k}$ of equation (3) with $i+j+k = n$.

The first two nonvanishing tensor moments for CH_4 are the octopole (2^3-pole) and hexadecapole (2^4-pole) moments; these tensor moments each have one independent component, conventionally [33] taken to be

$$\Omega = M_{xyz} = \tfrac{5}{2} P_{1,1,1} \tag{5}$$

for the octopole moment and

$$\Phi = M_{xxxx} = \tfrac{7}{4} \left(P_{4,0,0} - 3P_{2,2,0} \right) \tag{6}$$

for the hexadecapole moment. From the results given in Table 1, we obtain HF ab initio values for these moments of $\Omega = 2.436$ au and $\Phi = -7.781$ au using the atom-centered Gaussian basis sets mentioned previously. These values are in good agreement with those obtained by Maroulis [34] ($\Omega = 2.409$ au and $\Phi = -7.690$ au) using a comparable, but not identical atom-centered basis set. Electron correlation effects on Ω and Φ are apparently relatively small, as the coupled-cluster values obtained from the results in Table 1 are $\Omega = 2.533$ au and $\Phi = -7.650$ au.

4 Electrostatic interactions between CH_4 and MgO(100)

We now consider the electrostatic interaction between the (frozen) charge distribution of the CH_4 molecule and the electric field $\mathbf{F} = -\nabla\varphi$ above the MgO(100) surface. If the charge distributions of the CH_4 molecule and the MgO(100) surface do not overlap, this electrostatic interaction is given by

$$V_{\mathrm{es}} = -\sum_\alpha F_\alpha M_\alpha - \frac{1}{3}\sum_{\alpha\beta} F_{\alpha\beta} M_{\alpha\beta} - \frac{1}{15}\sum_{\alpha\beta\gamma} F_{\alpha\beta\gamma} M_{\alpha\beta\gamma} - \frac{1}{105}\sum_{\alpha\beta\gamma\delta} F_{\alpha\beta\gamma\delta} M_{\alpha\beta\gamma\delta} - \cdots \tag{7}$$

where the Greek-letter subscripts symbolize Cartesian directions x, y, and z in the aforementioned coordinate system originating at the C nucleus. In this equation,

$$F_\alpha = -\frac{\partial\varphi}{\partial r_\alpha} \tag{8}$$

represents a Cartesian component of the electric field, and the field gradients $F_{\alpha\beta}$ and $F_{\alpha\beta\gamma}$ are defined as

$$F_{\alpha\beta} = -\frac{\partial^2\varphi}{\partial r_\alpha \partial r_\beta} \quad \text{and} \quad F_{\alpha\beta\gamma} = -\frac{\partial^3\varphi}{\partial r_\alpha \partial r_\beta \partial r_\gamma} \tag{9}$$

with a straightforward generalization to $F_{\alpha\beta\gamma\delta}$ and higher-order field gradients. In equations (8) and (9), the components and gradients of the field $\mathbf{F}$ are evaluated at the carbon nucleus of the CH_4 molecule. The prefactor associated with the 2^n-pole term in equation (7) is $-1/(2n-1)!!$

To take advantage of the simplifications afforded by the standard orientation for CH_4, we must transform $\varphi(X, Y, Z)$ [Eq. (1)] into the (x, y, z) coordinate system defined by the CH_4 standard orientation before evaluating the electric field and its gradients. Suppose that an edge-down CH_4 adsorbate is stationed above a surface-layer Mg ion and oriented so that its surface-directed CH bonds are in the $Y = 0$ plane. In this case, we have

$$X = (x + y)/\sqrt{2} \tag{10}$$

$$Y = (x - y)/\sqrt{2} \tag{11}$$

$$Z = h + z \tag{12}$$

where h is the adsorption height, defined as the distance between the C nucleus and the $Z = 0$ MgO(100) plane. For a face-down CH_4 adsorbate stationed above a surface-layer Mg ion and oriented so that one surface-directed CH bond resides in the $Y = 0$ plane, we choose the MgO surface normal to be aligned with the CH bond that points in the $(x, y, z) = (1, 1, 1)$ direction. Then we have

$$X = \big(2z - x - y\big)/\sqrt{6} \tag{13}$$

$$Y = \big(x - y\big)/\sqrt{2} \tag{14}$$

$$Z = h + \big(x + y + z\big)/\sqrt{3}. \tag{15}$$

Substituting equations (10) through (12) or (13) through (15) into equation (1) and differentiating with respect to the Cartesian coordinates x, y, and z gives the field gradients needed to evaluate the electrostatic interaction energy $V_{\rm es}$ using equation (5) when CH_4 is held in its standard orientation.

Performing this computation and retaining terms through the 2^8-pole moment of CH_4, we find that for the edge-down CH_4 adsorbate,

$$V^{(8)}_{\rm es,edge} = \frac{Q}{4\pi\epsilon_0}\frac{128\sqrt{2}}{3}\left(\frac{e^{-\sqrt{8}\pi h/a}}{1+e^{-\pi\sqrt{2}}}\right)\left(U_{4,0,0} - 3U_{2,2,0} + \frac{4}{105}U_{8,0,0} - \frac{16}{15}U_{6,2,0} + \frac{4}{3}U_{4,4,0}\right) \tag{16}$$

where we have defined $U_{i,j,k} = (P_{i,j,k}/a)(\pi/a)^{i+j+k}$ for the sake of conciseness, and the superscript (8) indicates that the expression given is correct through the 2^8-pole moment. For the face-down CH_4 adsorbate,

$$V^{(8)}_{\rm es,face} = \frac{Q}{4\pi\epsilon_0}\frac{32}{9}\left(\frac{e^{-\sqrt{8}\pi h/a}}{1+e^{-\pi\sqrt{2}}}\right) \times\left(-20\sqrt{3}U_{1,1,1} - 7\sqrt{2}U_{4,0,0} + 21\sqrt{2}U_{2,2,0} + \frac{16\sqrt{2}}{45}U_{6,0,0} - 16\sqrt{2}U_{4,2,0} + 32\sqrt{2}U_{2,2,2} + \frac{208\sqrt{3}}{9}U_{3,3,1} + \frac{11\sqrt{2}}{105}U_{8,0,0} - \frac{44}{15}U_{6,2,0} + \frac{11}{3}U_{4,4,0}\right). \tag{17}$$

The leading terms (through the 2^4-pole moment) of equations (16) and (17) can be simplified by recalling the definitions of Ω and Φ given in equations (5) and (6):

$$V^{(4)}_{\rm es,edge} = \frac{Q}{4\pi\epsilon_0}\frac{512\sqrt{2}\pi^4\Phi}{21a^5}\left(\frac{e^{-\sqrt{8}\pi h/a}}{1+e^{-\pi\sqrt{2}}}\right) \tag{18}$$

and

$$V^{(4)}_{\rm es,face} = -\frac{Q}{4\pi\epsilon_0}\frac{128}{9}\left(\frac{2\sqrt{3}\pi^3\Omega}{a^4} + \frac{\sqrt{2}\pi^4\Phi}{a^5}\right)\left(\frac{e^{-\sqrt{8}\pi h/a}}{1+e^{-\pi\sqrt{2}}}\right). \tag{19}$$

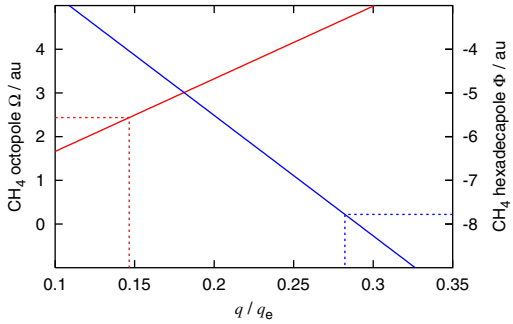

Fig. 3. Dependence of the CH_4 octopole moment Ω and the hexadecapole moment Φ on the hydrogen effective charge q for a point-charge model of CH_4. Horizontal dotted lines indicate the Hartree-Fock ab initio values for Ω and Φ obtained in this work.

For a point-charge model of CH_4 in its standard orientation,

$$\Omega = \frac{10qb^3}{3\sqrt{3}} \qquad \text{and} \qquad \Phi = -\frac{14qb^4}{9} \tag{20}$$

where q is the effective charge of the H atoms. Figure 3 shows how the Ω and Φ values for the point-charge model depend on q when the CH bond length b is fixed at its equilibrium value [24]. This figure, and equations (18) and (19), help us understand the shortcomings of a point-charge model for the CH_4 charge distribution.

The CH_4 octopole moment Ω makes no contribution to the electrostatic interaction $V_{\rm es,edge}$ for edge-down CH_4 adsorbates, and the leading term in $V_{\rm es,edge}$ is proportional to the CH_4 hexadecapole moment Φ. For face-down adsorbates, on the other hand, both Ω and Φ contribute to the electrostatic interaction $V_{\rm es,face}$. Because Φ is negative (see Fig. 3), it stabilizes the edge-down configuration and destabilizes the face-down configuration. Because Ω is positive, it stabilizes the face-down configuration (and makes no contribution to the energy of the edge-down configuration).

Figure 3 shows that if the partial charge q on the hydrogen atoms of CH_4 is chosen so as to reproduce the CH_4 octopole moment ($q \approx 0.15q_{\rm e}$), as was done in references [5,14], the resulting hexadecapole moment will be almost 50% too small. In this case, the leading term in $V_{\rm es,edge}$ will also be underestimated by roughly 50%, as will the destabilizing hexadecapolar contribution to $V_{\rm es,face}$ for the face-down configuration. The net result is that the binding of the face-down CH_4 adsorbate to the MgO(100) surface will be artificially strengthened, while the binding of the edge-down adsorbate to the MgO(100) surface will be artificially weakened. For the empirical CH_4–MgO(100) interaction potentials used in references [5,14], this provides enough additional relative stability to the face-down adsorption configuration to make it the minimum energy configuration.

Figure 4 compares the electrostatic coefficients s for edge-down and face-down CH_4 molecules with substrate-charge-normalized electrostatic interactions $V_{\rm es}/Q$ computed from equations (16) and (17), using the HF multipole moments of Table 1. We see that the interaction

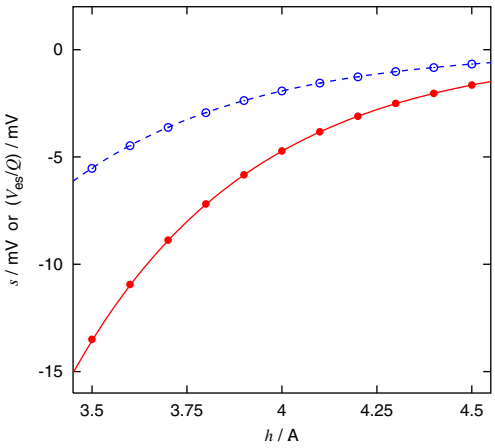

Fig. 4. Dependence on the CH_4 height h of both the ab initio CH_4–lattice electrostatic interaction coefficient s and the substrate-charge-normalized interaction V_{es}/Q given by equations (16) and (17). Open and filled circles represent s for face-down and edge-down adsorbates, respectively; dashed and solid curves represent V_{es}/Q for face-down and edge-down adsorbates, respectively.

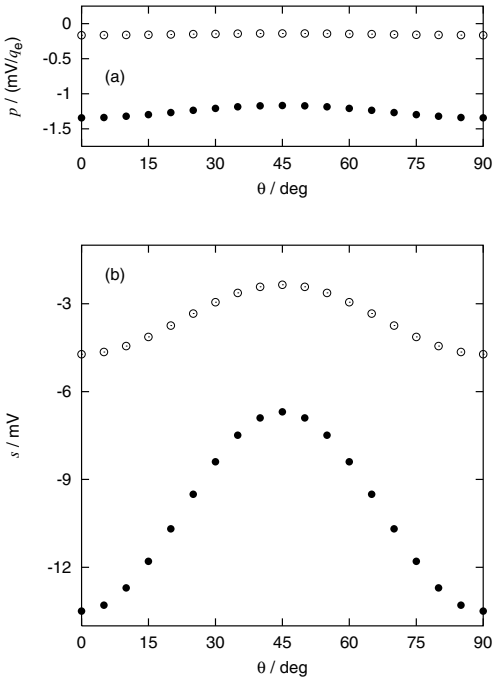

Fig. 5. Variation of the ab initio CH_4–lattice induction interaction coefficient p (panel a) and electrostatic interaction coefficient s (panel b) as an edge-down CH_4 molecule at height $h = 3.5$ Å (filled circles) or 4.0 Å (open circles) rotates around the surface normal; θ is the angle between the X-axis and a line through the two downward-pointing H atoms.

energies given by these two equations are in excellent agreement with those obtained from the ab initio calculations, indicating that (at least for the h range studied here) CH_4 multipoles beyond the 2^8-pole moment make insignificant contributions to the CH_4–lattice interaction for the two adsorption configurations studied here. At $h = 3.5$ Å, the truncated V_{es} expressions given in equations (18) and (19) give interaction energies that are respectively 1% and 37% larger than those obtained using the more complete expressions in equations (16) and (17). This indicates that while the hexadecapolar term in V_{es} is overwhelmingly dominant for edge-down CH_4 molecules, higher order CH_4 multipoles (particularly the 2^6- and 2^7-pole moments) make significant contributions to V_{es} for face-down CH_4 adsorbates.

5 Rotational barriers for edge-down CH_4 molecules

Recent experimental studies [13,16,18] of the CH_4–MgO(100) system have focused on the rotational dynamics of the CH_4 adsorbate molecules. These molecules (whether edge-down or face-down) each have 12 equivalent adsorption configurations, distinguished solely by permutations of the H atoms, and linked by 120° and 180° rotations around the CH_4 molecule's symmetry axes. Because energetic barriers inhibit free rotation of the adsorbate around these symmetry axes, the adsorbates exhibit tunneling splittings associated with the "jumps" among these equivalent configurations. An analysis of the experimentally-observed tunneling splittings for CH_4 adsorbates on MgO(100) suggests that the molecules adopt the edge-down adsorption configuration [18].

A first-principles simulation of these tunneling splittings would provide further insight into the relationship between the splittings and the underlying adsorbate-substrate interaction potential; however, such a simulation requires an accurate six-dimensional CH_4–MgO(100) potential energy surface, which is not yet available. Nevertheless, an examination of the physical origin of the energetic barriers to CH_4 adsorbate rotation could help us both understand the tunneling splittings in more detail, and extract useful information from them. We therefore use the ab initio protocol outlined above to quantify the electrostatic and induction components of the barrier to rotation, about the surface normal, of edge-down CH_4 adsorbates positioned at fixed height above the point charge bilayer. Our results for adsorbates at $h = 3.5$ Å and 4.0 Å, computed at the HF level of theory, are shown in Figure 5.

For an isolated edge-down CH_4 molecule above the point charge bilayer, a 90° rotation about the surface normal returns the CH_4 molecule to an energetically degenerate configuration, as is obvious in Figure 5. In the real CH_4/MgO(100) monolayer, this degeneracy may be broken by lateral CH_4–CH_4 interactions [19], in which case a rotation of 180° would be required for the CH_4 adsorbate to revisit an equivalent configuration. However, if the CH_4–MgO(100) and CH_4–CH_4 interactions are pairwise additive (or nearly so), the electrostatic and induction *components* of the rotational barriers that are depicted in Figure 5 will carry over into the full CH_4–MgO(100) interaction potential.

What this figure indicates is that at $h = 3.5$ Å, the electrostatic component of the interaction gives rise

to a substantial barrier to rotation of edge-down CH_4 molecules about the surface normal. The induction component of the interaction, on the other hand, varies only weakly as the CH_4 molecule rotates about this axis. Because the dipole-dipole polarizability tensor α for CH_4 is isotropic, induction contributions associated with α are invariant to reorientation of the CH_4 molecule; the weak angular corrugation observed in Figure 5a must therefore arise from higher order polarizabilities of CH_4 such as the dipole-quadrupole or quadrupole-quadrupole polarizabilities. What is clear from Figure 5, however, is that induction effects arising from polarization of CH_4 adsorbates by the MgO(100) near-surface electric field will probably make only minor contributions to the barrier to rotation of edge-down adsorbates about the surface normal. (While the calculations summarized in Figure 5 have been done only at the HF level, electron correlation effects on the anisotropic polarizabilities of CH_4 appear to be relatively small [34], so that the inclusion of these effects should not change this conclusion.)

6 Discussion

In this work, we have used ab initio quantum chemical methods to investigate the electrostatic interaction between a CH_4 adsorbate molecule and a finite lattice of point charges intended to mimic the MgO(100) surface. We find that the CH_4 molecule adsorbs above a positive surface-layer ion, and that the edge-down adsorption configuration is substantially more stable than the face-down configuration. This is in contrast to the prediction of empirical CH_4–MgO(100) interaction potentials that use a point-charge model to represent the charge distribution of the CH_4 adsorbate; as we have shown, this discrepancy can be understood through an analysis of the electrostatic component of the CH_4–MgO(100) interaction in terms of the multipole moments of the CH_4 adsorbate.

Of what relevance is this work for the real CH_4–MgO(100) system? The results shown in Figure 4 suggest that for Q values close to $2q_e$ (representing a fully ionic MgO solid) and adsorption heights near 3.5 Å (which is close to the adsorption heights predicted in Refs. [15, 19]), the electrostatic component of the CH_4–MgO(100) interaction potential should contribute about 25 meV to the CH_4 adsorption energy for edge-down CH_4 adsorbate molecules. As we mentioned previously, the analysis presented here is quantitatively accurate only when the adsorbate and substrate charge distributions do not overlap; for the real CH_4–MgO(100) system, or for quantum chemical calculations which treat the electronic structure of the MgO(100) substrate explicitly, the electrostatic contribution to the adsorption energy will be reduced somewhat because of interpenetration of the CH_4 and MgO(100) charge distributions.

To assess the magnitude of these interpenetration effects, we can compare our purely electrostatic estimates of the CH_4 adsorption energy to the adsorption energies obtained from a molecular orbital quantum chemical calculation that included the substrate electronic structure explicitly [15]. In this calculation, the MgO(100) surface was represented by a small cluster of Mg and O ions directly underneath the CH_4 adsorbate (one surface-layer Mg^{2+} ion and its five nearest-neighbor O^{2-} ions); these ions were surrounded by an array of ab initio model potentials which was then embedded in a Madelung potential representing the rest of the MgO(100) substrate. The CH_4 adsorption energy was computed at the HF and modified coupled pair functional (MCPF) levels of theory; the HF calculations used a CH_4 atom-centered basis set somewhat smaller than the one employed here. In this study, the HF CH_4–MgO(100) binding energy was computed to be about 2 meV; calculations using a larger basis set at the MCPF level gave a computed CH_4 binding energy of about 40 meV, which rose to about 55 meV after empirical adjustment to account for incompleteness in the one- and many-electron basis sets.

The HF CH_4 adsorption energy obtained from this ab initio calculation should already encompass nearly all of the electrostatic component of the CH_4-substrate interaction; however, the ab initio adsorption energy differs by an order of magnitude from the purely electrostatic estimate obtained here for a hypothetical fully ionic MgO substrate. One possible explanation for this discrepancy is that the interpenetration effects described above are substantial for adsorption heights near 3.5 Å. But these effects should also be present in the density functional theory (DFT) studies [19] of CH_4 adsorption on MgO(100), studies which predict a per-molecule adsorption energy of 18 meV for "herringbone" monolayers of CH_4 [22]. This latter per-molecule adsorption energy estimate is in qualitative agreement with our purely electrostatic estimate. It thus seems unlikely that our neglect of interpenetration effects is responsible for the order-of-magnitude disagreement with the adsorption energy obtained in the HF calculation.

Furthermore, DFT studies of bare MgO(100) surfaces [35] suggest that the surface-layer Mg ions carry an effective partial charge of $Q \approx 1.7q_e$; because the electrostatic component of the CH_4–MgO interaction scales linearly with Q, using this value for Q gives an electrostatic contribution to the CH_4–MgO(100) binding energy of about 21 meV. This value is in semi-quantitative agreement with the value obtained in the DFT calculation, suggesting that dispersion interactions make a fairly small contribution to the DFT-computed CH_4–MgO binding energy. (This is not to say that dispersion interactions are unimportant in the *real* CH_4–MgO system, only that these interactions play a minor role in promoting CH_4 adsorption in the DFT-simulated system. The failure of the DFT protocol used in Ref. [19] to predict the physisorption of CH_4 on Ir surfaces [36] suggests that this protocol probably underestimates the magnitude of dispersion interactions.)

One notable difference between the HF calculation [15] and the DFT calculation [19] is that the latter calculation employs periodic boundary conditions. Periodic HF calculations of CH_4 adsorption on MgO(100) might therefore help resolve the discrepancies between these calculations,

and could also help quantify the extent to which the DFT studies actually do incorporate dispersion interactions.

This work was partially supported by the Air Force Office of Scientific Research through grant F-49620-01-1-0068. We thank Prof. J.Z. Larese for several helpful discussions and Dr. M.L. Drummond for sharing some pre-publication results with us. Basis sets were obtained from the Extensible Computational Chemistry Environment Basis Set Database ⟨`http://www.emsl.pnl.gov/forms/basisform.html`⟩ developed and distributed by the Molecular Science Computing Facility of the Environmental and Molecular Sciences Laboratory (EMSL). EMSL is part of the Pacific Northwest Laboratory (PNL, P.O. Box 999, Richland, WA 99352, USA) and is funded by the US Department of Energy. PNL is a multi-program laboratory operated by Battelle Memorial Institute for the US Department of Energy under contract DE-AC06-76RLO 1830. Contact Karen Schuchardt for further information about the Basis Set Database.

References

1. B. Deprick, A. Julg, Chem. Phys. Lett. **110**, 150 (1984)
2. B. Deprick, A. Julg, Nouv. J. Chem. **11**, 299 (1987)
3. C. Girard, C. Girardet, Chem. Phys. Lett. **138**, 83 (1987)
4. D.R. Jung, J. Cui, D.R. Frankl, G. Ihm, H.Y. Kim, M.W. Cole, Phys. Rev. B **40**, 11893 (1989)
5. A. Alavi, Mol. Phys. **71**, 1173 (1990)
6. A. Lakhlifi, C. Girardet, Surf. Sci. **241**, 400 (1991)
7. D.R. Jung, J. Cui, D.R. Frankl, Phys. Rev. B **43**, 10042 (1991)
8. J.Z. Larese, J.M. Hastings, L. Passell, D. Smith, D. Richter, J. Chem. Phys. **95**, 6997 (1991)
9. J.M. Gay, P. Stocker, D. Degenhardt, H.J. Lauter, Phys. Rev. B **46**, 1195 (1992)
10. L.M. Quattrocci, G.E. Ewing, J. Chem. Phys. **96**, 4205 (1992)
11. D. Smith, Chem. Phys. Lett. **228**, 379 (1994)
12. J. Heidbert, O. Schonekas, H. Weiss, G. Lange, J.P. Toennies, Ber. Bun. **99**, 1370 (1995)
13. J.Z. Larese, Physica B **248**, 297 (1998)
14. S. Picaud, C. Girardet, T. Duhoo, D. Lemoine, Phys. Rev. B **60**, 8333 (1999)
15. K. Todnem, K.J. Børve, M. Nygren, Surf. Sci. **421**, 296 (1999)
16. A. Freitag, J.Z. Larese, Phys. Rev. B **62**, 8360 (2000)
17. K.A. Davis, G.E. Ewing, J. Chem. Phys. **113**, 10313 (2000)
18. J.Z. Larese, D. Martin y Marero, D.S. Sivia, C.J. Carlile, Phys. Rev. Lett. **87**, 206102 (2001)
19. M.L. Drummond, B.G. Sumpter, W.A. Shelton, J.Z. Larese, Phys. Rev. B **73**, 195313 (2006)
20. J.P. Perdew, J.A. Chevary, S.H. Vosko, K.A. Jackson, M.R. Pederson, D.J. Singh, C. Fiolhais, Phys. Rev. B **46**, 6671 (1992)
21. J.P. Perdew, J.A. Chevary, S.H. Vosko, K.A. Jackson, M.R. Pederson, D.J. Singh, C. Fiolhais, Phys. Rev. B **48**, 4978 (1993)
22. M.L. Drummond, private communication (2006)
23. W.A. Steele, *The Interaction of Gases with Solid Surfaces* (Pergamon, Oxford, 1974)
24. D.L. Gray, A.G. Robiette, Mol. Phys. **37**, 1901 (1979)
25. M.J. Frisch et al., Gaussian 03, Revision B.05 (Gaussian, Inc., Pittsburgh, PA, 2003)
26. T.H. Dunning Jr, J. Chem. Phys. **90**, 1007 (1989)
27. R.A. Kendall, T.H. Dunning Jr, R.J. Harrison, J. Chem. Phys. **96**, 6769 (1992)
28. D.E. Woon, T.H. Dunning Jr, J. Chem. Phys. **103**, 4572 (1995)
29. T. Helgaker et al., DALTON, a molecular electronic structure program, Release 1.2.1, ⟨`http://www.kjemi.uio.no/software/dalton/dalton.html`⟩ (2001)
30. J. Cizek, Adv. Chem. Phys. **14**, 35 (1969)
31. G.D. Purvis, R.J. Bartlett, J. Chem. Phys. **76**, 1910 (1982)
32. G.E. Scuseria, C.L. Janssen, H.F. Schaefer III, J. Chem. Phys. **89**, 7382 (1988)
33. A.D. Buckingham, in *Intermolecular Interactions: From Diatomics to Biopolymers*, edited by B. Pullman (Wiley, New York, 1978)
34. G. Maroulis, Chem. Phys. Lett. **226**, 420 (1994)
35. U. Birkenheuer, J.C. Boettger, N. Rösch, J. Chem. Phys. **100**, 6826 (1994)
36. G. Henkelman, H. Jónsson, Phys. Rev. Lett. **86**, 664 (2001)